typeset using JPSJ.sty <ver.1.0b>

arXiv:cond-mat/0103530v1 [cond-mat.str-el] 26 Mar 2001

Crossover from Quarter-Filling to Half-Filling in a One-Dimensional Electron System with a Dimerized and Quarter-Filled Band*

Masahisa Tsuchiizu,[1]** Hideo Yoshioka[2] and Yoshikazu Suzumura[1,3]

[1] *Department of Physics, Nagoya University, Nagoya 464-8602*
[2] *Department of Physics, Nara Women's University, Nara 630-8506*
[3] *CREST, Japan Science of Technology Corporation (JST)*

(Received)

The interplay between quarter-filled and half-filled umklapp scattering has been examined by applying the renormalization group method to a one-dimensional quarter-filled electron system with dimerization, on-site (U) and nearest-neighbor (V) repulsive interactions. The phase diagram on the U-V plane is obtained at absolute zero temperature where the Mott insulator (the charge ordered insulator) is found for smaller (larger) V. By choosing the moderate parameter in the region of Mott insulator, it is shown that the resistivity exhibits a crossover from behavior of quarter-filling to that of half-filling with decreasing temperature.

KEYWORDS: quarter-filling, dimerization, half-filling, umklapp scattering, Bechgaard salts

The organic conductors, Bechgaard salts, which show a crystal structure with a stacking of organic molecules along one-dimensional axis, form a quasi-one-dimensional system with a quarter-filled hole band.[1,2] Recently, the states above the phase transition temperature have been studied extensively to show several experimental observations which may be relevant to the unconventional non-Fermi liquid. Optical and photoemission experiments exhibit the charge gap in both TMTTF salts and TMTSF salts.[3,4] The charge ordered (CO) insulating state in (TMTTF)$_2$AsF$_6$ and (TMTTF)$_2$PF$_6$ has been maintained by the NMR measurement[5] and the huge dielectric response in (TMTTF)$_2$PF$_6$[6] indicates also the CO state. It is necessary to understand these experimental facts in consistent with a general phase diagram of the Bechgaard salts indicating a dimensional crossover.[7]

Two mechanisms for the insulating state has been proposed theoretically.[8] One is of them is the half-filled umklapp scatterings induced by dimerization[9] and the charge gap has been examined for the one-dimensional quarter-filled Hubbard model with the dimerization.[10] The other is the commensurability at the quarter-filling. The quarter-filled extended Hubbard model without the dimerization has been examined by using a method of numerical diagonalization, where the phase diagram shows the insulating state with the charge gap for a large Coulomb repulsion.[11,12] The similar phase diagram has been obtained analytically by calculating the magnitude of the umklapp scattering at quarter-filling and by using the bosonization method and the renormalization group technique.[13,14] The model treating both of these two umklapp scattering on the same footing is required for investigating Bechgaard salts. By using the DMRG method, the charge gap of the model has been estimated where the metallic state is reduced to the insulator in the presence of dimerization.[16]

In the present letter, we investigate the interplay of the half-filled umklapp scattering and the quarter-filled one by extending the previous work[13,14] to the case including the dimerization. It is demonstrated that the competition between these two scatterings gives rise to two-kinds of unconventional insulating states in the ground state and that a crossover between these two states appears in the resistivity at finite temperatures.

We consider a one-dimensional quarter-filled extended Hubbard model with dimerization. The Hamiltonian is given by

$$\mathcal{H} = -\sum_{j,\sigma}\left(t+(-1)^j t_{\rm d}\right)\left(c^\dagger_{j,\sigma}c_{j+1,\sigma}+{\rm h.c.}\right) + U\sum_j n_{j,\uparrow}n_{j,\downarrow} + V\sum_j n_j n_{j+1} \ , \qquad (1)$$

where $n_{j,\sigma}=c^\dagger_{j,\sigma}c_{j,\sigma}$ and $n_j=n_{j,\uparrow}+n_{j,\downarrow}$. The fermion operator $c^\dagger_{j,\sigma}$ denotes a creation of the electron at the j-th site with spin σ. We have two kinds of transfer integrals $t+t_{\rm d}$ and $t-t_{\rm d}$ due to the dimerization. The quantities U and V denote the on-site and nearest-neighbor Coulomb repulsive interaction. In the presence of the dimerization, the unit cell is given by two lattice sites with $2a$ where a is the lattice constant. By introducing operators $c^A_{R_n,\sigma}$ and $c^B_{R_n+a,\sigma}$ which are those for the even and odd sites in the n-th unit cell ($R_n=2an$), respectively, we perform the Fourier transform $c^A_{k,\sigma}=N_0^{-1/2}\sum_n^{N_0}{\rm e}^{-ikR_n}\,c^A_{R_n,\sigma}$ and $c^B_{k,\sigma}=N_0^{-1/2}\sum_n^{N_0}{\rm e}^{-ik(R_n+a)}\,c^B_{R_n+a,\sigma}$, where $N_0=L/(2a)$ and L is the length of the system. Then the kinetic term of the Hamiltonian, $\mathcal{H}_0$, is diagonalized as $\mathcal{H}_0=\sum_{k,\sigma}\varepsilon_k\,[d^\dagger_{k,\sigma}d_{k,\sigma}-u^\dagger_{k,\sigma}u_{k,\sigma}]$ with a dispersion relation, $\varepsilon_k=-2[t^2\cos^2 ka+t_{\rm d}^2\sin^2 ka]^{1/2}$. In a diagonalized basis, the lower and upper band fermion operators are given by $d_{k,\sigma}=[{\rm e}^{i\theta_k}\,c^A_{k,\sigma}+{\rm e}^{-i\theta_k}\,c^B_{k,\sigma}]/\sqrt{2}$ and

---

* submitted to J. Phys. Soc. Jpn.

** E-mail: tsuchiiz@edu2.phys.nagoya-u.ac.jp

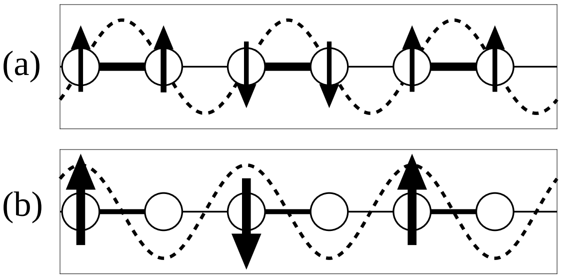

Fig. 1. Schematic view of the two limiting cases for the insulating state: the Mott insulating state (a) and the CO insulating state (b). The dashed wave indicates the $4k_{\rm F}$ charge density wave with $\theta_\rho = \pi/4$ (a) and $\theta_\rho = 0$ or $\pi/2$ (b).

$u_{k,\sigma} = [{\rm e}^{i\theta_k}\, c^A_{k,\sigma} - {\rm e}^{-i\theta_k}\, c^B_{k,\sigma}]/\sqrt{2}$, respectively, where $\tan 2\theta_k = -(t_{\rm d}/t)\tan ka$. Since a gap $4t_{\rm d}$ appears at $k = \pm\pi/2a$ and the first Brillouin zone is reduced to half, the system can be regarded effectively as half-filling with $k_{\rm F} = \pi/4a$.

In order to obtain the effective Hamiltonian for the states near $\pm k_{\rm F}$, one integrates out the contribution from the upper band, which leads to the quarter-filled umklapp scattering.[13)] We apply the bosonization method to electrons in the lower band with the dispersion linearized as $\varepsilon_k \to \pm v_{\rm F}(|k| - k_{\rm F})$ where $v_{\rm F} = \sqrt{2}ta[1-(t_{\rm d}/t)^2]/[1+(t_{\rm d}/t)^2]^{1/2}$. Then the Hamiltonian, which is rewritten in terms of the charge and spin phase variable, is decoupled into two parts of the charge and spin degrees of freedom. The charge part, $\mathcal{H}_\rho$, is expressed as[15)]

$$\begin{aligned}\mathcal{H}_\rho = \frac{v_\rho}{4\pi}\int {\rm d}x \left[\frac{1}{K_\rho}\left(\partial_x\theta_\rho\right)^2 + K_\rho\left(\partial_x\phi_\rho\right)^2\right] \\ - \frac{g_{1/2}}{2\pi^2\alpha^2}\int {\rm d}x\, \sin 2\theta_\rho \\ + \frac{g_{1/4}}{2\pi^2\alpha^2}\int {\rm d}x\, \cos 4\theta_\rho \ ,\end{aligned} \tag{2}$$

where α is a cutoff of the order of lattice constant and $[\theta_\rho(x), \phi_\rho(x')] = i\pi\,{\rm sgn}(x-x')$. In eq. (2), the charge velocity and the Tomonaga-Luttinger exponent are given by $v_\rho = v_{\rm F}[(1+g_{4\rho}/2\pi v_{\rm F})^2 - (g_\rho/2\pi v_{\rm F})^2]^{1/2}$ and $K_\rho = [(2\pi v_{\rm F} + g_{4\rho} - g_\rho)/(2\pi v_{\rm F} + g_{4\rho} + g_\rho)]^{1/2}$. The magnitude of half-filled umklapp scattering, $g_{1/2}$, and that of quarter-filled one, $g_{1/4}$, are given by

$$g_{1/2} = B\left[Ua - \frac{Aa^2}{2\pi v_{\rm F}}U\,(U-2V)\,I_2(A)\right] \ , \tag{3}$$

$$g_{1/4} = \frac{1}{(2\pi\alpha)^2}\,\frac{A^4\,a^5}{v_{\rm F}^2}\,U^2(U-4V) \ , \tag{4}$$

where $A \equiv [1-(t_{\rm d}/t)^2]/[1+(t_{\rm d}/t)^2]$ and $B \equiv [2t_{\rm d}/t]/[1+(t_{\rm d}/t)^2]$. The quantity $g_{1/4}$ has been derived for $t_{\rm d} = 0$.[13)] The constants g_ρ and $g_{4\rho}$ are given by[13)]

$$\begin{aligned}g_\rho &= (U+4V)a \\ &\quad - \frac{Aa^2}{4\pi v_{\rm F}}\Big[(U-2V)^2 + U^2 + (2V)^2\Big]\,I_1(A) \ , \\ g_{4\rho} &= (U+4V)a \\ &\quad - \frac{Aa^2}{4\pi v_{\rm F}}\Big[(U-2V)^2 + U^2B^2 + (2V)^2\Big]\,I_2(A) \ ,\end{aligned}$$

where $I_1(A) \equiv \int_0^{\pi/2}{\rm d}\varphi\, \sum_{\epsilon=\pm}[2+2\sqrt{1+\epsilon A\cos\varphi}]^{-1}$, and $I_2(A) \equiv 2\int_0^{\pi/2}{\rm d}\varphi\, [2+\sqrt{1+A\cos\varphi}+\sqrt{1-A\cos\varphi}]^{-1}$. These quantities are calculated as $I_1(A) \simeq I_1(1) = \ln(\sqrt{2}+1)$ and $I_2(A) \simeq I_2(1) = 2(\sqrt{2}+1)$. The order parameters of the $4k_{\rm F}$ charge density wave (CDW) state is given by[13)]

$$\mathcal{O}_{4k_{\rm F}\text{-CDW}} \propto \cos\left(4k_{\rm F}x + 2\theta_\rho\right) \ . \tag{5}$$

From eq. (2), one finds the following facts. In the case of $g_{1/4} = 0$, θ_ρ is locked to $\theta_\rho = \pi/4$ for $g_{1/2} > 0$, (or $\theta_\rho = 3\pi/4$ for $g_{1/2} < 0$) with $0 \le \theta_\rho < \pi$. In this case, the charge configuration for $4k_{\rm F}$-component is shown schematically in Fig. 1(a), which corresponds to the Mott insulating state. We note that the sign of the half-filled umklapp scattering depends on that of the dimerization, i.e., $g_{1/2} > 0$ for $t_{\rm d} > 0$ and $g_{1/2} < 0$ for $t_{\rm d} < 0$. On the other hand, in the case of $g_{1/2} = 0$, the phase is locked to $\theta_\rho = 0$, $\pi/2$ for $g_{1/4} < 0$ or $\theta_\rho = \pi/4$, $3\pi/4$ for $g_{1/4} > 0$. The locking of θ_ρ for $g_{1/4} < 0$ (i.e., $U < 4V$) corresponds to the CO insulating state shown in Fig. 1(b). In the presence of both $g_{1/2}$ and $g_{1/4}$, the behavior becomes quite different depending on the sign of $g_{1/4}$. In the case, $g_{1/4} > 0$, the two kinds of umklapp scattering are compatible and $g_{1/2}$-term removes the degeneracy between $\theta_\rho = \pi/4$ and $\theta_\rho = 3\pi/4$. However, in $g_{1/4} < 0$ case, the two kinds of umklapp scattering compete with each other since the locking positions of θ_ρ are different for respective umklapp scattering. The CO state, which appears in large V, has been obtained by the mean-field approximation method[17)] and the competition between these two kinds of potentials has been shown in terms of phase variable.[18)] Here we investigate the competition between the Mott insulator and the CO insulator, by employing the renormalization group method, where the quantum fluctuation is fully taken into account.

The renormalization group equations for the coupling constants in the Hamiltonian, eq. (2), are given by

$$\frac{\rm d}{{\rm d}l}\,K_\rho = -2\,G_{1/2}^2\,K_\rho^2 - 8\,G_{1/4}^2\,K_\rho^2 \ , \tag{6}$$

$$\frac{\rm d}{{\rm d}l}\,G_{1/2} = (2-2K_\rho)\,G_{1/2} + G_{1/2}\,G_{1/4} \ , \tag{7}$$

$$\frac{\rm d}{{\rm d}l}\,G_{1/4} = (2-8K_\rho)\,G_{1/4} + \frac{1}{2}\,G_{1/2}^2 \ , \tag{8}$$

where $G_z = g_z/(2\pi v_\rho)$ $(z = 1/2,\ 1/4)$ and $l = \ln(\alpha'/\alpha)$ with the new length scale α' being larger than α. We note that these renormalization group equations can be derived in a way similar to Ref. 19. Equations (7) and (8) indicate the fact that $G_{1/2}$ and $G_{1/4}$ are suppressed by each other for $G_{1/4} < 0$ and are enhanced for $G_{1/4} > 0$ as discussed in the last paragraph.

The competition for $g_{1/4} < 0$ (i.e., $U < 4V$) is examined numerically. The parameter of the dimerization is taken as $t_{\rm d}/t$ =0.001 to show results clearly, although such a choice is rather small compared with that of the organic conductors ($t_{\rm d}/t \simeq 0.1$). In Fig. 1, the l-dependences of $K_\rho(l)$, $G_{1/2}(l)$ and $G_{1/4}(l)$ are shown for $U/t = 6$ and

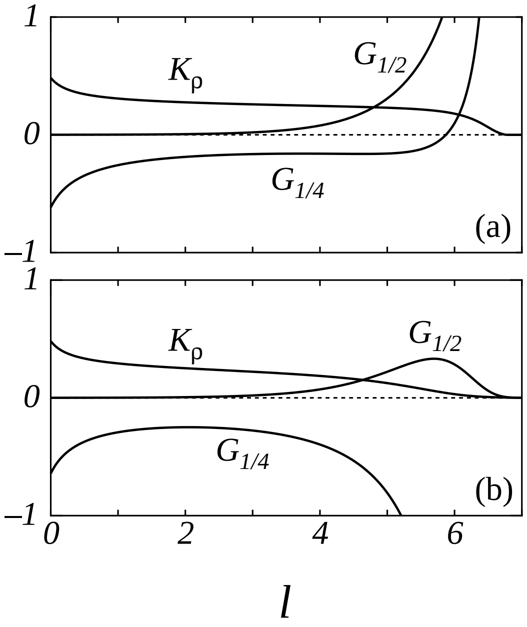

Fig. 2. The scaling flows of the coupling constants for $V/t = 4.60$ (a) and 4.75 (b) where $U/t = 6$ and $t_\mathrm{d}/t = 0.001$. These are the typical scaling flows for the Mott insulator (a) and for the CO insulator (b), respectively.

$t_\mathrm{d}/t = 0.001$ with fixed $V/t = 4.60$ (a) and 4.75 (b). For both cases, the exponent K_ρ decreases monotonically indicating the insulating state. In Fig. 1(a), the half-filled umklapp scattering $G_{1/2}(l)$ increases and becomes relevant leading to the Mott insulator. The sign of $G_{1/4}(l)$ changes from negative to positive due to the relevant $G_{1/2}(l)$. Figure 1(b) exhibits $G_{1/2}(l)$ and $G_{1/4}(l)$, which are quite different compared with those of Fig. 1(a). In this case, $G_{1/4}(l)$ is relevant while $G_{1/2}(l)$ decreases after taking a maximum and becomes irrelevant. The relevance of $G_{1/4}$ with negative value denotes the locking of θ_ρ being 0 or $\pi/2$ and leading to the CO insulating state.

Based on Fig. 2, the phase diagram of the ground state is shown in Fig. 3 with fixed $t_\mathrm{d}/t = 0.001$. In the Mott insulator, the phase θ_ρ is locked at $\theta_\rho = \pi/4$, while in the CO insulator the phase is fixed at $\theta_\rho = 0$ or $\pi/2$. The dashed curve denotes the boundary in the limit of $t_\mathrm{d} \to 0$, which is equal to that of the metal-insulator transition in the quarter-filled extended Hubbard model.[13] In the presence of t_d, the metallic region for $t_\mathrm{d} = 0$ changes into the Mott insulating state and the CO insulating region is suppressed. At the boundary, the charge configuration changes from uniform (Fig.1(a)) to CO (Fig.1(b)) with increasing V. We note that the state at the boundary becomes metallic since this case corresponds to an Ising transition found in the sine-Gordon system with two kinds of non-linear terms, i.e., the gap collapses on the criticality.[20, 21, 22]

Now we examine the competition at finite temperatures. We calculate the temperature dependence of the resistivity using the memory functional approach[23, 24] which has been applied to the one-dimensional systems by Giamarchi.[25] The conductivity is given by $\sigma(\omega) = i[\chi(\omega) - \chi(0)]/\omega$, where χ is the retarded

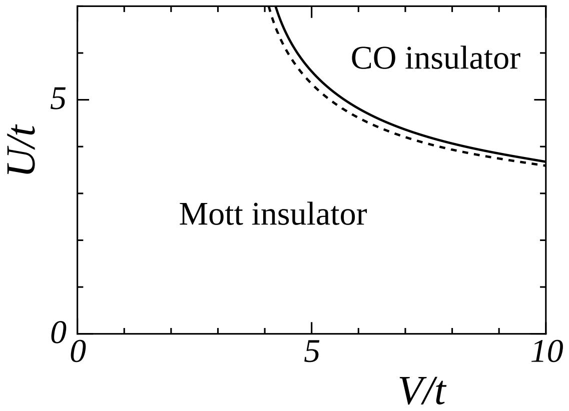

Fig. 3. The phase diagram of the Mott insulator and the CO insulator on the plane of U/t and V/t with fixed $t_\mathrm{d}/t = 0.001$. The dashed curve indicates the boundary in the limit of $t_\mathrm{d} \to 0$.

current-current correlation function: $\chi(\omega) \equiv \langle\langle j; j\rangle\rangle_\omega \equiv -i\int dx \int_0^\infty dt\, \langle[j(x,t),\, j(0,0)]\rangle\, e^{i\omega t-\delta t}$. The current operator $j(x,t)$ is given by $j(x,t) = -\partial_t\theta_+(x,t)/\pi = -2v_\rho K_\rho\,\Pi(x,t)$ where $\Pi \equiv -\partial_x\theta_-/(2\pi)$. From the memory function approach, $\sigma(\omega)$ is rewritten as[25]

$$\sigma(\omega) = i\,\frac{2v_\rho K_\rho}{\pi}\,\frac{1}{\omega + M(\omega)}\ , \tag{9}$$

where $M(\omega)$ is the memory function defined by $M(\omega) \equiv \omega\,\chi(\omega)/[\chi(0) - \chi(\omega)]$. The memory function is calculated perturbatively as $M(\omega) \simeq -[\langle\langle F; F\rangle\rangle^0_\omega - \langle\langle F; F\rangle\rangle^0_{\omega=0}]/[\omega\chi(0)]$ where $\langle\langle F; F\rangle\rangle^0_\omega$ stands for the retarded correlation function in the absence of umklapp scattering and $F \equiv [j, \mathcal{H}]$. In terms of $M(\omega)$, the resistivity is expressed as

$$\rho(T) = \lim_{\omega\to 0}\sigma^{-1}(\omega) = \frac{\pi}{i2v_\rho K_\rho}\lim_{\omega\to 0} M(\omega)\ . \tag{10}$$

Equation (10) indicates the power-law behavior,

$$\rho(T) \propto \sum_{n=1,2} G^2_{1/2n}\, T^{4n^2K_\rho - 3}\ . \tag{11}$$

In order to obtain the precise behavior of the resistivity, we use the solutions of the renormalization group equations, in which the umklapp scattering becomes relevant at low temperature. By putting $e^{-l} = 2\pi T/W$ with $W \equiv v_\rho\alpha^{-1}$, the resistivity is obtained as

$$\rho(T) = \sum_{n=1,2}\frac{4n^2\pi}{\alpha}\, G^2_{1/2n}(l)\,\cos^2\left(n^2\pi K_\rho(l)\right) \times B^2\left(n^2K_\rho(l), 1 - 2n^2K_\rho(l)\right)\, e^{-l}\ . \tag{12}$$

where $B(x,y)$ is the beta function given by $B(x,y) \equiv \Gamma(x)\Gamma(y)/\Gamma(x+y)$. In Fig. 4, the temperature dependence of the resistivity is shown for $U/t = 6$ and $t_\mathrm{d}/t = 0.001$ with fixed $V/t = 4.60$ (a) and 4.75 (b). The curve (a) shows the behavior of the Mott insulator, while the curve (b) represents that of the CO insulator. For the CO insulator (curve (b)), the resistivity is determined by the quarter-filled umklapp scattering, where the resistivity exhibits the power-law dependence given by $\rho(T) \propto T^{16K_\rho - 3}$ around the temperature $T/W \gtrsim 1\times 10^{-1}$. The temperature $T/W \simeq 5\times 10^{-2}$,

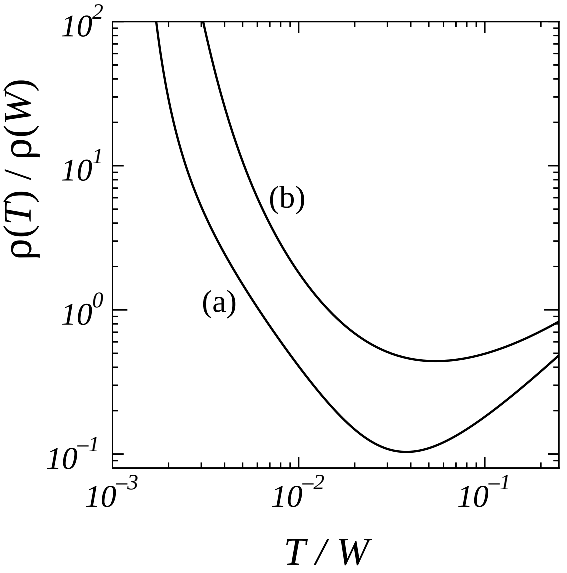

Fig. 4. The temperature dependence of the resistivity for $U/t = 6$ and $t_{\rm d}/t = 0.001$with fixed $V/t = 4.60$ (a) and 4.75 (b) where W denotes the cutoff of the order of the bandwidth. The curve (a) (curve (b)) corresponds to the behavior of the Mott insulator (the CO insulator).

corresponding to a minimum of the resistivity, is of the order of the charge gap Δ_ρ below which the resistivity increases rapidly. It is expected that the resistivity for $T \ll \Delta_\rho$ behaves as $\exp(\Delta_\rho/T)$,[8] although the perturbative renormalization group approach breaks down for $T \ll \Delta_\rho$. For the case of the Mott insulator (curve (a)), we found a noticeable behavior due to the relevance of the half-filled umklapp scattering. There appears a mid temperature region around $T/W \simeq 1 \times 10^{-2}$, where the resistivity shows power-law behavior of half-filling given by $\rho(T) \propto T^{4K_\rho - 3}$. At higher temperatures ($T/W \gtrsim 4 \times 10^{-2}$), the contribution of the quarter-filled umklapp scattering becomes dominant at which the resistivity is similar to the case of curve (b). Such a crossover in the region of CO insulator can be found by the moderate choice of parameter with $|G_{1/4}| > G_{1/2}$, i.e., close to the boundary in Fig. 3. The similar result is found in the frequency dependence of the conductivity at $T = 0$. While the optical conductivity of the CO insulating phase corresponding to curve (b) shows the power-law dependence with $\sigma(\omega) \propto \omega^{16K_\rho - 5}$ above the frequency of the charge gap, the conductivity of the Mott insulator corresponding to curve (a) shows a crossover from $\sigma(\omega) \propto \omega^{16K_\rho - 5}$ to $\sigma(\omega) \propto \omega^{4K_\rho - 5}$ as decreasing frequency. Thus, the crossover from quarter-filling to half-filling is found with decreasing temperature or frequency when parameters are located in the Mott insulating region and close to the boundary.

Finally we comment on observation in the Bechgaard salts, (TMTTF)$_2$X and (TMTSF)$_2$X. The optical measurement in the normal states of these salts shows that the optical conductivity has a power-law dependence as $\sigma(\omega) \propto \omega^{-1.3}$ at high frequency, indicating a fact that the quarter-filled umklapp scattering is dominant.[26] Our calculation suggests that the quarter-filled umklapp scattering becomes always dominant at high frequency when the parameter is close to the boundary. Therefore the power-law dependence of the optical conductivity $\sigma(\omega) \propto \omega^{16K_\rho - 5}$ could be compatible with the charge gap, which originates in the Mott insulator and/or the CO insulator.

In conclusion, we found two kinds of insulator, the Mott insulator and the CO insulator, for the ground state of a one-dimensional quarter-filled system with dimerization, where the half-filled umklapp scattering induced by the dimerization competes with the quarter-filled umklapp scattering for large nearest-neighbor Coulomb interaction $V (> U/4)$. In the Mott insulating phase close to the boundary, the half-filled umklapp scattering is dominant at low T but the quarter-filled umklapp scattering becomes dominant at high T, and then the resistivity could exhibit a crossover from a quarter-filled behavior to a half-filled one as decreasing temperature.

Acknowledgements

The authors would like to thank E. Orignac for discussion on the resistivity and also H. Seo for useful comments.

---

[1] D. Jérome and H.J. Schulz: Adv. Phys. **31** (1982) 299; K. Bechgaard and D. Jérome: Physica Scripta **T39** (1991) 37.
[2] G. Grüner: Rev. Mod. Phys. **66** (1994) 1.
[3] A. Schwartz, S. Donovan, M. Dressel, L. Degiorgi and G. Grüner: Synth. Met. **86** (1997) 2129.
[4] V. Vescoli, L. Degiorgi, W. Henderson, G. Grüner, K. P. Sarkey and L. K. Montgomery: Science **281** (1998) 1181.
[5] D.S. Chow, F. Zamborszky, B. Alavi, D.J. Tanillo, A. Baur, C.A. Merlic and S.E. Brown: Phys. Rev. Lett. **85** (2000) 1698.
[6] F. Nad, P. Monceau, C. Carcel and J.M. Fabre, Phys. Rev. B **62** (2000) 1753.
[7] J. Moser, M. Gabay, P. Auban-Senzier, D. Jérome, K. Bechgaard and J.M. Fabre: Eur. Phys. J. B **1** (1988) 39.
[8] T. Giamarchi: Physica B **230-232** (1997) 975.
[9] V. J. Emery, R. Bruinsma and S. Barišić: Phys. Rev. Lett. **48** (1982) 1039.
[10] K. Penc and F. Mila: Phys. Rev. B **50** (1994) 11429.
[11] F. Mila and X. Zotos: Europhys. Lett **24** (1993) 133.
[12] K. Sano and Y. Ōno: J. Phys. Soc. Jpn. **63** (1994) 1250.
[13] H. Yoshioka, M. Tsuchiizu and Y. Suzumura: J. Phys. Soc. Jpn. **69** (2000) 651, and references therein.
[14] H. Yoshioka, M. Tsuchiizu and Y. Suzumura: J. Phys. Soc. Jpn. **70** (2000) No. 3,
[15] M. Tsuchiizu: Ph.D. thesis at Nagoya University (2001).
[16] S. Nishimoto, M. Takahashi, Y. Ohta: J. Phys. Soc. Jpn. **69** (2000) 1594.
[17] H. Seo and H. Fukuyama: J. Phys. Soc. Jpn. **66** (1997) 1249.
[18] Y. Suzumura: J. Phys. Soc. Jpn. **66** (1997) 3244.
[19] M. Tsuchiizu and Y. Suzumura: J. Phys. Soc. Jpn. **68** (1999) 3966.
[20] G. Delfino and G. Mussardo: Nuclear Physics B **516** (1998) 675.
[21] M. Fabrizio, A. O. Gogolin and A. A. Nersesyan: Phys. Rev. Lett. **83** (1999) 2014, Nuclear Physics B **580** (2000) 647.
[22] The correspondence to the present model has been pointed out by E. Orignac.
[23] H. Mori: Prog. Theor. Phys. **33** (1965) 423, *ibid* **34** (1965) 399.
[24] W. Götze and P. Wölfle: Phys. Rev. B **6** (1972) 1226.
[25] T. Giamarchi: Phys. Rev. B **46** (1992) 342.
[26] A. Schwartz, M. Dressel, G. Grüner, V. Vescoli, L. Degiorgi and T. Giamarchi: Phys. Rev. B **58** (1998) 1261.